electronics

MDPI

Article

Cognitive Workload Classification in Industry 5.0 Applications: Electroencephalography-Based Bi-Directional Gated Network Approach

Muhammad Abrar Afzal [1,*], Zhenyu Gu [1,*], Bilal Afzal [2] and Syed Umer Bukhari [3]

[1] School of Design, Minhang Campus, Shanghai Jiao Tong University, Shanghai 200040, China
[2] School of Management & Economics, Qingshuihe Campus, University of Electronic Science and Technology of China, Chengdu 611731, China; bilal.afzal@outlook.com
[3] School of Computer Science & Technology, Changchun University of Science and Technology, Changchun 130022, China; umershah81@hotmail.com
* Correspondence: abrar456@sjtu.edu.cn (M.A.A.); zygu@sjtu.edu.cn (Z.G.)

Abstract: In the era of Industry 5.0, effectively managing cognitive workload is crucial for optimizing human performance and ensuring operational efficiency. Using an EEG-based Bi-directional Gated Network (BDGN) approach, this study tries to figure out how to classify cognitive workload in Industry 5.0 applications. The proposed approach incorporates LSTM (Long Short-Term Memory) and GRU (Gated Recurrent Unit) models in a hybrid architecture to leverage their complementary strengths. This research highlights the utilization of the developed model alongside the MQTT (Message Queuing Telemetry Transport) protocol to facilitate real-time end-to-end data transmission. The deployed AI model performs the classification of cognitive workload based on the received data. The main findings of this research reveal an impressive accuracy of 98% in cognitive workload classification, validating the efficacy of the suggested BDGN approach. This study emphasizes the significance of leveraging EEG-based approaches in Industry 5.0 applications for cognitive workload management.

Keywords: cognitive workload; Industry 5.0; electroencephalogram; bi-directional gated networks; human–robot interaction; artificial intelligence

check for updates

Citation: Afzal, M.A.; Gu, Z.; Afzal, B.; Bukhari, S.U. Cognitive Workload Classification in Industry 5.0 Applications: Electroencephalography-Based Bi-Directional Gated Network Approach. *Electronics* **2023**, *12*, 4008. https://doi.org/10.3390/electronics12194008

Academic Editor: Dimitris Apostolou

Received: 8 August 2023
Revised: 18 September 2023
Accepted: 18 September 2023
Published: 23 September 2023

1. Introduction

Industry 5.0 is set to usher in a new era of seamless integration between advanced technologies and human–machine interactions [1], increasing productivity and efficiency [2]. This paradigm shift emphasizes the optimization of human–machine interactions to improve overall performance [3]. A key aspect of this optimization is managing the cognitive workload placed on individuals [4] during their interactions with machines. Cognitive workload refers to the mental effort and resources required to accomplish a task or process information [5] effectively. It is influenced by task complexity [6], time pressure, and environmental demands [7]. Excessive cognitive workload can decrease performance and lead to errors and safety hazards [8]. Therefore, accurately assessing and managing the cognitive workload is crucial for optimizing human performance and ensuring safety in Industry 5.0 applications [9].

For real-time cognitive workload classification, various methods have been explored [10], including physiological measurements such as electroencephalography (EEG), which is a test that records the electrical activity of the brain using scalp electrodes [11]; electrocardiography (ECG), a medical test to measure the electrical activity of the heart [12]; electromyography (EMG), which is used to evaluate the electrical activity of muscles [13]; and eye tracking, which is technology that monitors and records the movement of the gaze of a person [14]. Task performance metrics [15], functional Near-Infrared Spectroscopy (fNIRS) [16],

and multimodal integration contribute further. Among the array of methods, electroencephalography (EEG) emerges as both a widely adopted and valuable approach [17]. EEG signals provide insights into the temporal dynamics of cognitive workload [18], enabling accurate assessment and classification in real-time scenarios [19].

Notably, EEG excels as a premier technique for real-time cognitive workload classification due to its direct brain activity measurement, high temporal resolution that captures rapid changes, noninvasiveness, portability, and sensitivity to nuanced cognitive states. These inherent advantages position EEG as a valuable tool to unravel the intricate neural dynamics of cognitive processes, making it pivotal for accurate and timely workload assessment across diverse real-world applications.

In the field of cognitive workload classification, there is a need for more research on how to combine EEG-based methods with more-advanced neural network architectures. While the significance of cognitive workload management is acknowledged, the existing methods often lack the precision and real-time capabilities required to meet the intricate demands of Industry 5.0 interactions. Most of the potential synergy between EEG signals and recurrent neural networks like LSTM and GRU is not being used. This leaves a hole in the field of efficient and accurate assessment of cognitive workload.

A research gap emerges in the realm of cognitive workload classification, specifically concerning the amalgamation of EEG-based methodologies with advanced neural network architectures. While the significance of cognitive workload management is acknowledged, the existing methods often lack the precision and real-time capabilities required to meet the intricate demands of Industry 5.0 interactions. The potential synergy between EEG signals and recurrent neural networks like LSTM and GRU remains largely untapped, leaving a void in the domain of efficient and accurate cognitive workload assessment.

In this study, we specifically focus on EEG as the primary method for cognitive workload classification. By leveraging EEG signals, we aim to extract meaningful features and patterns that correlate with different levels of cognitive workload. EEG allows us to capture the neural activity associated with cognitive processes [20], providing valuable information for real-time cognitive workload classification. Furthermore, EEG-based classification models have demonstrated promising performance in previous studies, showcasing their effectiveness in accurately assessing cognitive workload levels. Artificial intelligence techniques, such as Convolutional Neural Network (CNN) [21], Long Short-Term Memory (LSTM) [22], and Bi-directional Long Short-Term Memory (Bi-LSTM) [23], have shown promise in processing and analyzing EEG signals for cognitive workload classification. These models capture temporal dependencies and extract meaningful features from EEG data [24].

This research article presents a novel real-time cognitive workload classification approach in Industry 5.0 applications. We leverage Bi-Directional Gated Networks (BDGNs) to accurately and efficiently classify cognitive workload levels. We intend to develop a hybrid methodology integrating deep learning models, including LSTM and GRU [25,26], as a BDGN framework. By leveraging these models and the STEW dataset [27], our goal is to attain high accuracy in classifying various levels of cognitive workload.

To enable real-time classification in an industrial environment [28], our intended model is deployed alongside the MQTT [29] protocol. MQTT ensures efficient data transmission [30], facilitating timely cognitive workload classification. The north gateway receives EEG data forwarded to the server for cognitive workload classification. The resulting predictions are then transmitted to the south gateway for comprehensive analysis and informed decision-making. The remarkable effectiveness of the BDGN approach in real-time cognitive workload classification is emphasized by the findings of this research. Achieving a high classification accuracy of 98% demonstrates the potential of this approach to optimize industrial processes and enhance human–machine interactions. These findings underscore the significance of cognitive workload classification in industrial applications, emphasizing its impact on operational efficiency and safety. Effective cognitive workload classification in Industry 5.0 can enhance human–machine interactions and efficiency in

applications like manufacturing lines (task optimization) and telemedicine (accurate diagnostics), ensuring safer and more-productive operations [31]. By leveraging the power of EEG signals and the capabilities of the BDGN model, this research contributes to advancing cognitive workload classification and provides a solid foundation for designing and implementing intelligent systems that can adaptively respond to the cognitive demands of Industry 5.0 applications.

The remainder of this paper is organized as follows: Section 2 provides an overview of related work in cognitive workload classification. Section 3 describes the materials and methods, including the EEG data acquisition process, preprocessing techniques, and the architecture of the recommended BDGN model. Section 4 presents the results and discussion. Finally, Section 5 concludes the paper and provides future research directions.

2. Literature Review

Cognitive workload classification is crucial for optimizing human–machine interactions in various domains, including Industry 5.0 [32]. The reviewed studies highlight the field's advancements, methodologies, and limitations, providing valuable insights for developing our research.

Shao et al. [33] proposed an EEG-based mental workload classification framework utilizing a combination of Bi-LSTM and ResNet models in an IoT scenario. They employed the STEW dataset and performed time–frequency analysis to extract informative features. The scheme achieved an accuracy of 90.64% for different tasks, demonstrating the effectiveness of their approach. Additionally, the authors evaluated the scheme for mental workload valuation and achieved an accuracy of 82.85%.

Gupta et al. [34], in their study, presented a subject-specific cognitive workload classification approach using EEG and deep learning models, specifically conv-LSTM. Their study involved 19 participants, and an accuracy of 93.75% was achieved. The researchers organized their own experiment at the Department of Biomedical Engineering, Institute of Nuclear Medicine and Allied Sciences, Delhi, India, showcasing the feasibility of their advocated approach in a controlled setting.

Keeping in view the importance of recurrent neural networks (RNNs), Chakladar et al. [23] introduced a novel framework for estimating different levels of mental workload using the gray wolf optimizer algorithm and a deep BLSTM-LSTM neural model. Their experiments involved "No task" and "multitasking activity" scenarios, achieving classification accuracies of 86.33% and 82.57%, respectively. However, it is worth noting that their approach did not incorporate transfer learning to other types of tasks, limiting its generalizability.

Kwak et al. [35] proposed an LSTM-based temporal attention technique to extract both local and global structure information from EEG data for mental workload classification. Their approach demonstrated remarkable accuracy, achieving 90.8% on their own dataset. Although their study did not focus specifically on IoT scenarios, the findings highlight the potential of temporal attention mechanisms for effective mental workload classification.

In another study, Wójcik et al. [36] focused on a three-class classification of cognitive workload using EEG data. They conducted their own experiment with 12 participants, analyzing the data from 11 subjects. Employing SVM, decision tree, k-NN, and random forest models, they achieved accuracies of 82.9%, 70.4%, 91.5%, and 84.6%, respectively.

While significant progress has been made in EEG-based cognitive workload classification for IoT scenarios, several research gaps need to be addressed. Firstly, there is a limited focus on cognitive workload classification in industrial applications, highlighting the need for tailored approaches to address the unique challenges and requirements of Industry 5.0. Additionally, existing models such as CNN, LSTM, and Bi-LSTM may not be efficient for real-time EEG data processing in resource-constrained IoT devices.

Furthermore, the transferability of models to different tasks and achieving high accuracy for industrial deployment require further investigation. Challenges related to varying environmental conditions, electrode placement variability, and subject-specific factors in

industrial scenarios also need to be explored to enhance the practical implementation of cognitive workload classification systems.

3. Materials and Methods

3.1. The Proposed Framework

This research study presents a deep learning model for real-time data transmission and classification. We utilized a publicly available dataset using IEEE DataPort [27] and conducted preprocessing steps to enhance the data quality and prepare the data for training our model [37]. Furthermore, we leveraged the MQTT (Message Queuing Telemetry Transport) protocol to enable end-to-end data transmission and classification with the deployed deep learning model. This section provides a comprehensive overview of the dataset, preprocessing, time domain analysis, power spectral density (PSD) analysis, and the deployment process, highlighting the critical steps involved in our research methodology.

Figure 1 depicts the proposed cognitive workload classification framework. The process initiates with the acquisition of raw EEG data, followed by preprocessing involving artifact removal, filtering, and segmentation. Post-preprocessing, the data undergo time domain and power spectral density (PSD) analysis to extract valuable characteristics. The preprocessed data are then fed into the BDGN model for classification. The model is deployed on a server. Simultaneously, the North gateway obtains EEG data from the STEW dataset, forwarding the data to an MQTT broker. The broker transmits the data to the server for live classification, and the results are relayed back to the broker. Finally, the broker shares the results, linking with the South gateway.

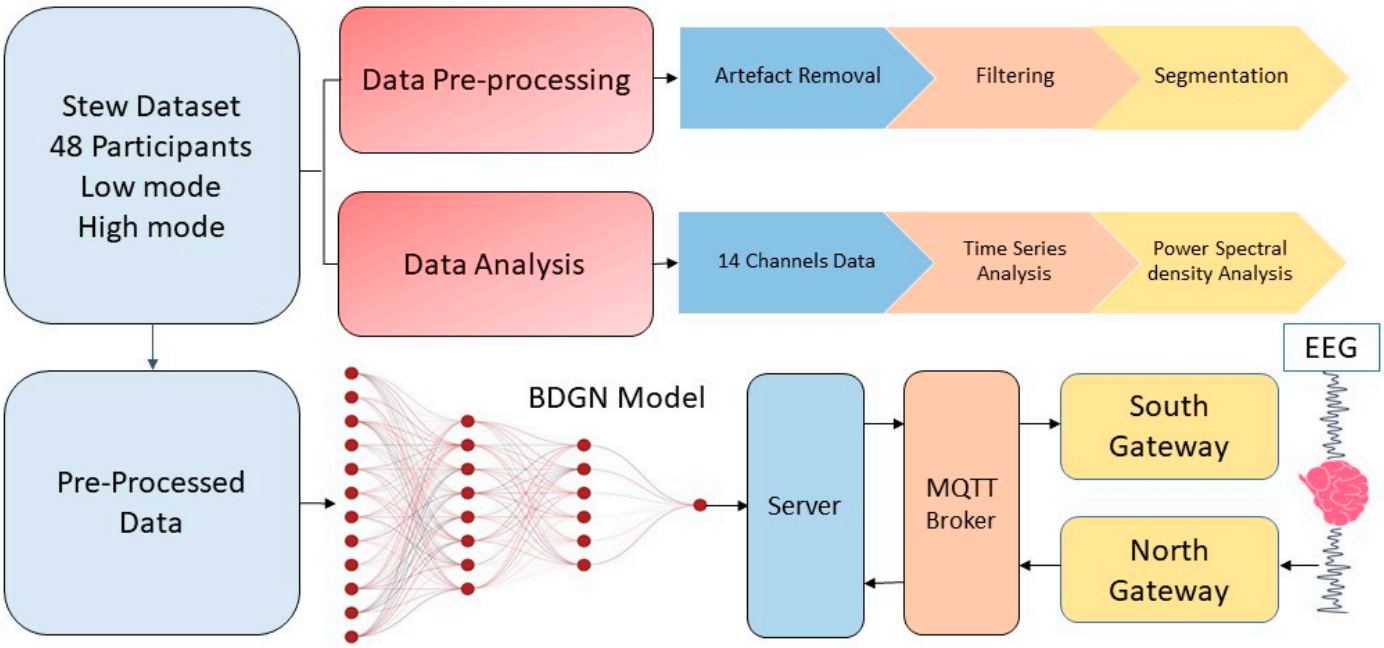

Figure 1. A framework of the proposed cognitive workload classification.

3.2. Dataset Description

The STEW (Simultaneous Task EEG Workload) is a publicly available dataset comprising EEG signals from 48 male subjects collected at Nanyang Technological University [23]. EEG data were captured using the Emotive EEG device. The recruited participants had no history of neurological or brain-related conditions and had not participated in prior EEG studies. The dataset encompasses EEG recordings in two distinct states: the rest state and the task execution state.

The rest state indicates periods when no specific tasks were performed, while the task execution state involved engaging in a multitasking test called SIMKAP. Each subject in the

dataset comprises 19,200 samples in both rest and task execution states. During SIMKAP, the participants were instructed to compare numbers in two windows, cross out matching numbers, and answer accompanying questions simultaneously.

Participants were also requested to provide subjective ratings of their perceived workload during the rest state and SIMKAP tasks. Equal task completion was ensured among all subjects during EEG data acquisition. SIMKAP, widely adopted for assessing multitasking stress [38], serves as a valuable component of this dataset.

3.3. Preprocessing

Each subject in the STEW dataset recorded 14 channels of EEG signals and sampled at a rate of 128 Hz, with a total recording time of 3 min per subject. To mitigate the influence of intertask activity, the initial 15 s and final 15 s of each signal were discarded, resulting in a final signal length of 2.5 min. The EEG signals dataset is preprocessed using the Python-based jupyterlab toolbox, and only signals within the frequency range of 0.5–100 Hz were retained for psychological load analysis [39].

The dataset categorized the EEG signals into two distinct tasks: the rest mode and the SIMKAP task. Ratings of mental workload levels, obtained from the subjects themselves, were used as labels for the different task phases. The ratings were classified into three levels: low workload (ratings 1–3), average workload (ratings 4–6), and high workload (ratings 7–9). The classification performance was assessed by comparing the predicted workload ratings with the actual labels of the unseen data.

3.4. Time Domain Analysis

Time domain analysis serves as a critical component of our study, involving an in-depth examination of EEG data acquired during both low-mode and high-mode conditions [40]. This analytical approach delves into the temporal intricacies of the EEG data, facilitating an exploration of distinctive patterns and fluctuations over time. To comprehensively understand the underlying dynamics, EEG data from both low-mode and high-mode conditions were leveraged for this analysis. Particularly, this method was applied across all 14 channels, offering a holistic overview of the temporal aspects and revealing potential insights into the intricate neural responses characteristic of these distinct cognitive states. This rigorous time domain analysis provides a foundation for elucidating the temporal dynamics of EEG data and contributes to our comprehensive investigation of cognitive workload classification.

Figure 2a,b depict the outcomes of our time domain analysis conducted on EEG data. We chose to focus on two specific channels, namely Channel 1 and Channel 14, as representative examples. While our comprehensive analysis encompasses all 14 channels, the selection of these two channels is intended to offer a succinct overview of the overarching trends observed in our study. Channel 1 represents the initial channel, while Channel 14 signifies the final channel in our dataset. This selection is not meant to diminish the significance of the other channels but serves to illustrate key findings within the constraints of this presentation. The analysis involved a comparison between two distinct conditions: Low-Mode and High-Mode cognitive workload conditions. In these figures, the x-axis corresponds to time, measured in seconds, while the y-axis represents the amplitude of the EEG signals.

The purpose of this analysis was to investigate how the EEG signals from these two channels vary over time under different cognitive workload conditions. Channel 1 and Channel 14 were selected as representative examples to showcase the observed patterns. By comparing the EEG signals between the Low-Mode and High-Mode conditions, we aimed to identify any notable differences in terms of signal amplitude and fluctuations.

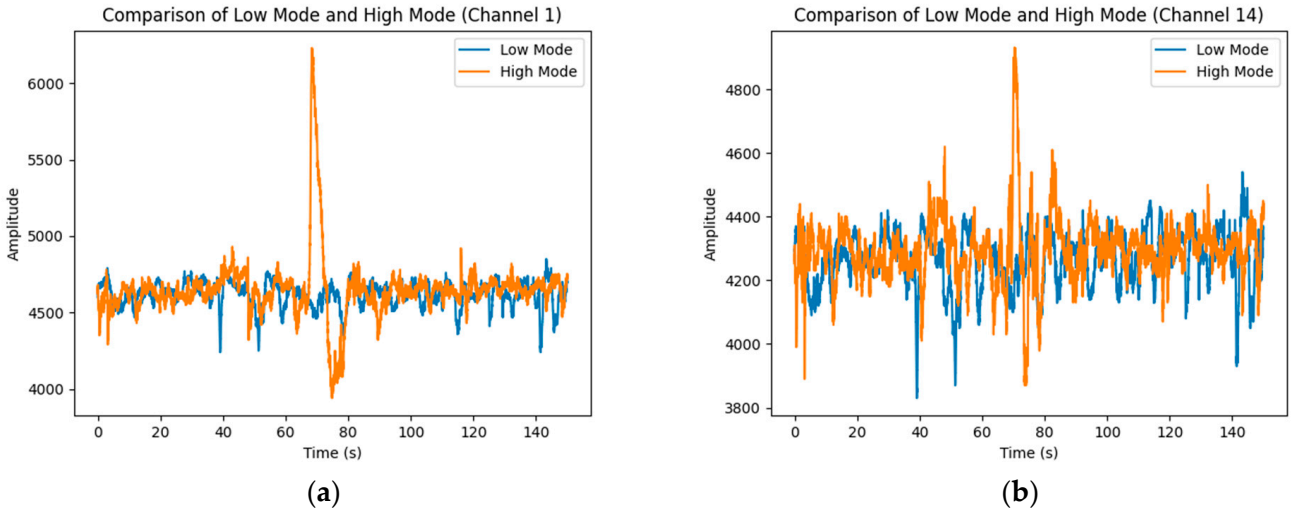

(**a**) (**b**)

Figure 2. (**a**,**b**) Time domain analysis.

3.5. Power Spectral Density (PSD) Analysis

The power spectral density (PSD) analysis is performed to understand EEG data's frequency characteristics and power distribution [41]. The raw EEG data for the low and high modes were obtained, and relevant channels were selected for further analysis. The sampling frequency of 128 Hz was used to process the data. Frequency bands of interest, including Delta (0.5–4 Hz), Theta (4–8 Hz), Alpha (8–13 Hz), Beta (13–30 Hz), and Gamma (30–100 Hz), were defined to explore brain activity patterns. The FFT algorithm was applied to compute the frequency components and their magnitudes. The power spectrum was then calculated by taking the absolute value squared of the FFT output [42], representing the distribution of power across different frequency components. Analysis was performed within each frequency band to quantify the power present in each respective range.

Here is the equation for the PSD of EEG signals:

$$PSD(f) = |\mathrm{FFT}(\mathrm{x(t)})\hat{}2/(\mathrm{T} * \mathrm{Fs}) \tag{1}$$

where PSD(f) is the power spectral density at frequency f,

FFT(x(t)) is the Fast Fourier Transform of the EEG signal x(t),

| FFT(x(t)) | ^2 represents the squared magnitude of the FFT,

T is the total duration of the EEG signal in seconds,

Fs is the sampling frequency of the EEG signal in Hz.

In Figure 3a,b, the power spectrum distribution analysis of EEG data is presented for both the Low-Mode and High-Mode cognitive workload conditions. The x-axis of these figures denotes different frequency bands, encompassing the Delta, Theta, Alpha, Beta, and Gamma ranges. Meanwhile, the y-axis signifies the corresponding power values associated with each frequency band. This analysis unveils how the power of EEG signals is distributed across different frequency components, offering insights into the distinctive neural activity patterns between the two cognitive workload conditions.

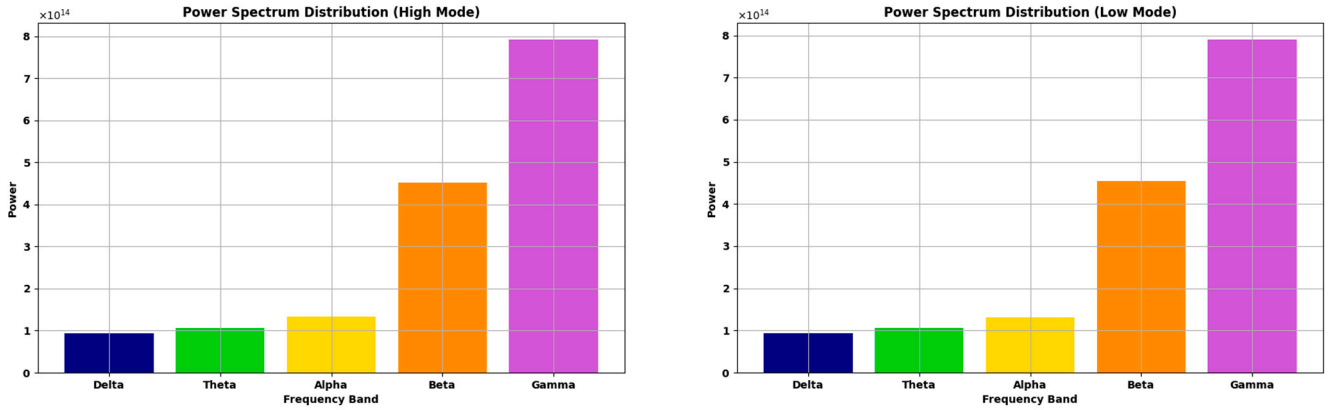

(**a**) (**b**)

Figure 3. (**a**,**b**) Frequency bands.

3.6. Deep Learning Model for Cognitive Workload Classification

The Bi-directional Gated Network (BDGN) introduces an innovative framework that effectively harnesses the synergistic capabilities of Long Short-Term Memory (LSTM) and Gated Recurrent Unit (GRU) neural networks to achieve precise cognitive workload classification. In BDGN, the LSTM and GRU components play pivotal roles in capturing and processing intricate temporal patterns within the EEG data.

3.6.1. BDGN Architecture

The architectural design of the BDGN model is meticulously sculpted within the Keras framework, where layers are carefully sequenced to optimize the performance. Beginning with an input layer, the architecture evolves into a 64-unit LSTM layer, adept at capturing intricate long-range dependencies courtesy of its inherent memory mechanism. After that, a GRU layer with 32 units is added without any problems. This makes the model better at figuring out complex temporal relationships, which are key to cognitive workload analysis. Culminating the architectural journey is a dense layer armed with a SoftMax activation function, which translates into predicted class probabilities for the distinct "low", "normal", and "high" workload categories. This architecture balances complexity and efficiency, making it suitable for real-time cognitive workload assessment and demonstrating competitive performance in experiments.

The architecture of our hybrid LSTM–GRU model for cognitive workload classification is depicted in Figure 4. It shows the input layer, the hidden layers, and the output layer.

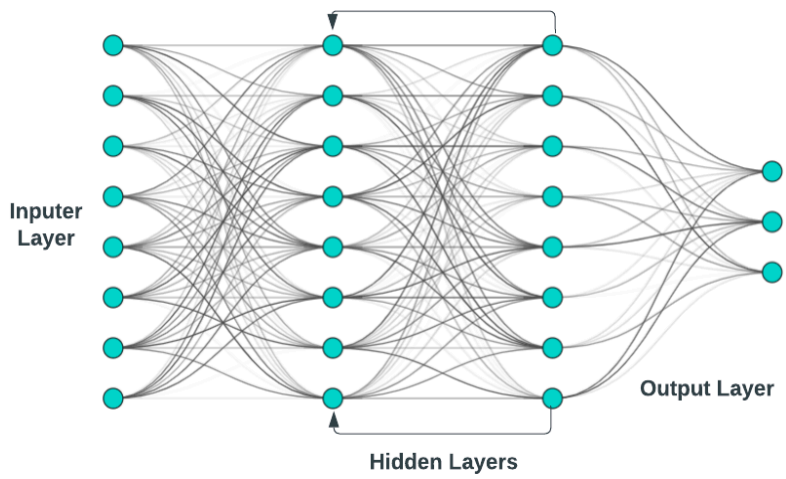

Figure 4. BDGN neural architecture.

3.6.2. BDGN Model Process

The input EEG data for the BDGN model consist of 96 files, divided into 48 low-mode and 48 high-mode data files. Each data file is structured as a matrix with dimensions of 19,200 rows (samples) and 15 columns. These columns encompass 14 EEG channels, and one additional column is allocated for ratings. The BDGN model processes the input EEG data (X_t) through the LSTM and GRU components step by step. Each step is defined by a mathematical equation as follows:

1. Input Gate (i_t):

The input gate (i_t) controls which values from the current input (X_t) and the previous hidden state (H_{t-1}^{LSTM}) should be incorporated into the cell state (C_t^{LSTM}).

$$i_t = \sigma\left(W_i \cdot \left[H_{t-1}^{LSTM}, X_t\right] + b_i\right) \tag{2}$$

Here, σ represents the sigmoid activation function, W_i is the weight matrix for the input gate, and b_i is the bias vector for the input gate.

2. Forget Gate (f_t):

The forget gate (f_t) determines what information from the previous LSTM cell state (C_{t-1}^{LSTM}) should be retained and what information should be discarded.

$$f_t = \sigma\left(W_f \cdot \left[H_{t-1}^{LSTM}, X_t\right] + b_f\right) \tag{3}$$

W_f is the weight matrix for the forget gate, and b_f is the bias vector for the forget gate.

3. Output Gate (o_t):

The output gate (o_t) determines what the next hidden state (H_t^{LSTM}) should be. It decides which parts of the current cell state (C_t^{LSTM}) should be revealed as the output.

$$o_t = \sigma\left(W_o \cdot \left[H_{t-1}^{LSTM}, X_t\right] + b_o\right) \tag{4}$$

W_o is the weight matrix for the output gate, and b_o is the bias vector for the output gate.

4. Update Cell State ($C_t^{candidate}$):

The update cell state ($C_t^{candidate}$) represents the candidate values that could potentially be updated in the cell state (C_t^{LSTM}).

$$C_t^{candidate} = tanh\left(W_c \cdot \left[H_{t-1}^{LSTM}, X_t\right] + b_c\right) \tag{5}$$

Here, *tanh* is the hyperbolic tangent activation function, W_c is the weight matrix for the candidate cell state, and b_c is the bias vector for the candidate cell state.

5. Update Cell State (C_t^{LSTM}):

The update cell state ($C_t^{Candidate}$) is combined with the forget gate (f_t) and the input gate (i_t) to compute the updated cell state (C_t^{LSTM}):

$$C_t^{LSTM} = f_t \cdot C_{t-1}^{LSTM} + i_t \cdot C_t^{candidate} \tag{6}$$

6. Hidden State (H_t^{LSTM}):

The final step in the LSTM layer computes the hidden state (H_t^{LSTM}) by applying the output gate (o_t) to the cell state (C_t^{LSTM}) after applying the hyperbolic tangent activation function:

$$H_t^{LSTM} = O_t \cdot \tanh\left(C_t^{LSTM}\right) \tag{7}$$

Now, using H_t^{LSTM} as the Input to the GRU Layer to Compute H_t^{GRU}, we obtain the following:

7. GRU Update Gate (z_t) and Reset Gate (r_t):

The GRU component employs the update gate (z_t) and the reset gate (r_t) to control how much of the previous hidden state (H_t^{LSTM}) is retained or updated and how much is forgotten when computing the candidate new hidden state.

$$z_t,\ r_t = \sigma\left(W_z \cdot \left[H_t^{LSTM}, X_t\right] + b_z,\ W_r \cdot \left[H_t^{LSTM}, X_t\right] + b_r\right) \tag{8}$$

8. GRU Candidate Hidden State ($H_t^{candidate}$):

The candidate hidden state ($H_t^{candidate}$) is calculated by applying the hyperbolic tangent activation function (*tanh*) to a weighted sum of $r_t \cdot H_t^{LSTM}$ and X_t.

$$H_t^{candidaate} = \tanh\left(W_h \cdot \left[r_t \cdot H_t^{LSTM}, X_t\right] + b_h\right. \tag{9}$$

9. Updated Hidden State of GRU (H_t^{GRU}):

The final updated hidden state (H_t^{GRU}) of the GRU layer is computed as a linear combination of $(1 - Z_t) \cdot H_t^{LSTM}$ and $Z_t \cdot H_t^{Candidate}$:

$$H_t^{Gru} = (1 - z_t) \cdot H_t^{LSTM} + Z_t \cdot H_t^{candidaate} \tag{10}$$

The input EEG data X_t are initially processed by the LSTM layer to obtain H_t^{LSTM}, and then H_t^{LSTM} is used as input to the GRU layer to compute the final updated hidden state H_t^{GRU}.

10. Output Prediction (Y_t):

The final prediction (Y_t) is computed using the updated hidden state (H_t^{GRU}) as input, followed by a SoftMax activation to obtain class probabilities.

$$Y_t = \text{Softmax}\left(W_y \cdot H_t^{GRU} + b_y\right) \tag{11}$$

These LSTM and GRU gates work synergistically in the BDGN, allowing the network to capture and process temporal dependencies at various time scales. The LSTM gates enable the model to manage long-term dependencies, while the GRU gates excel at capturing shorter-term patterns. The collaborative operation of these gates enhances the network's capacity to precisely classify cognitive workload levels based on EEG data, making the BDGN a promising advancement in cognitive workload assessment.

3.6.3. Data Partitioning and Model Training

To ensure both impartial evaluation and effective model training, a meticulous dataset partitioning scheme was devised, demarcating distinct subsets for dedicated training, validation, and rigorous testing. The partitioning strategy thoughtfully assigns 60% of the dataset to training, allocates 20% for validation, and carefully reserves 20% for the critical testing phase. For the training, we employed the Adam optimizer with a learning rate of 0.001, a popular choice for optimizing deep learning models. The sparse categorical cross-entropy loss function was used, which is well suited for multiclass classification tasks. Minimizing this loss function allows the model to assign high probabilities to the correct workload category during training. During the training process, the model was exposed to the training data for 50 epochs, this iterative learning process facilitates the model's progressive mastery of accurately classifying cognitive workload levels, resulting in heightened precision. The culmination of this iterative training led to the model's comprehensive evaluation, executed with rigor on the meticulously reserved testing set.

3.7. Evaluation Metrics and Measures

This research employed multiple evaluation metrics, including the confusion matrix. The confusion matrix provided a tabular representation of the model's performance, consisting of true labels (low, average, high) and predicted labels (low, average, high) obtained from the BDGN model. To assess the performance of the learning models, we employed key evaluation metrics, including accuracy [43], precision [44], recall [45], and F1-score [46]. These metrics provide comprehensive insights into the effectiveness of the models in classifying cognitive workload levels.

Accuracy is measured as follows:

$$Accuracy = \frac{True\ Positives + True\ Negatives}{Total\ Predictions} \tag{12}$$

Precision can be calculated as follows:

$$Precision = \frac{True\ Positives}{True\ Positives + False\ Positives} \tag{13}$$

To calculate the Recall, the below equation is used:

$$Recall = \frac{True\ Positives}{True\ Positives + False\ Negatives} \tag{14}$$

The F1-Score is measured as follows:

$$F1Score = 2 * \frac{Precision * Recall}{Precision + Recall} \tag{15}$$

3.8. Real-Time Cognitive Workload Classification

To achieve a comprehensive end-to-end solution encompassing data transmission and classification, the deployment seamlessly integrated the MQTT protocol with the BDGN model, harnessing MQTT QoS version 0, MQTT protocol 3.1.1, and the MQTT version EMQ X Broker Version 4.3.5. Through the MQTT protocol, efficient and reliable data communication [47] was facilitated between the North Gateway and South Gateway. The process unfolds as follows: the North Gateway acts as the data source, publishing EEG data to the MQTT broker, which, in turn, forwards the data to the AI script for real-time classification. Subsequently, the MQTT broker receives the classification results from the AI script. Concurrently, the South Gateway subscribes to the relevant topic, thereby receiving the classification results. Figure 5 shows the classification workflow, ensuring seamless data exchange across the network.

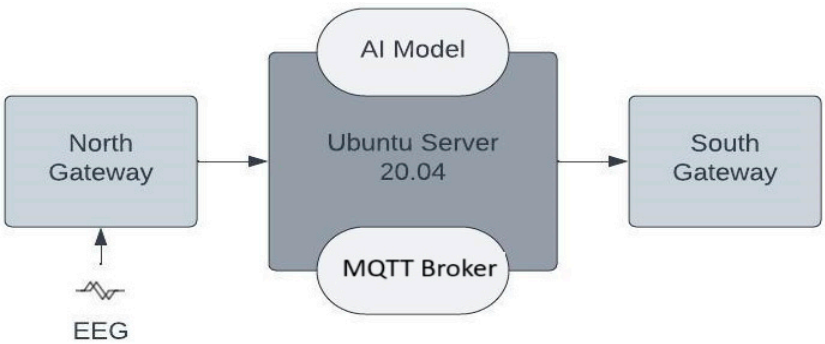

Figure 5. Illustration of real-time cognitive workload classification using BDGN model and MQTT protocol.

In the experimental scenario, the North Gateway continuously collected real-time EEG data at 128 Hz. These data were transmitted to the MQTT broker for immediate processing

and classification using the deployed BDGN model. The resulting classification labels, representing the cognitive workload levels (low, average, high), were sent to the South Gateway, enabling real-time access to the classified cognitive workload information.

This experimental setup allowed for the real-time monitoring and analysis of cognitive workload levels using the BDGN model and MQTT broker integration. By leveraging the BDGN model's power and the MQTT protocol's efficiency, this approach provided a robust and scalable solution for end-to-end cognitive workload classification in industrial applications.

4. Results and Discussion

This section presents the results obtained by implementing the BDGN model for real-time cognitive workload classification. Our study investigates the performance and effectiveness of the BDGN model in this specific task. We utilized performance metrics to evaluate the model's classification accuracy. Additionally, we compared our results with existing studies to assess the novelty and effectiveness of our approach. The presented findings contribute to our understanding of the BDGN model's capabilities and its potential for practical implementation in real-time cognitive workload classification.

4.1. Performance of Bi-Directional Gated Network (BDGN) Model

The BDGN (Bi-directional Gated Neural Network) model, which combines the LSTM (Long Short-Term Memory) and GRU (Gated Recurrent Unit) architectures, was implemented and evaluated for cognitive workload classification in real-time industrial applications. The model demonstrated exceptional performance, achieving a remarkable accuracy of 98%. Figure 6 presents the model accuracy plot, which provides insights into the performance of the BDGN model during training. The plot showcases consistently high accuracy across the training epochs, indicating the model's ability to classify cognitive workload levels accurately. The model achieved and maintained a remarkable accuracy level of 98%, highlighting its effectiveness in capturing the underlying patterns and characteristics of the data.

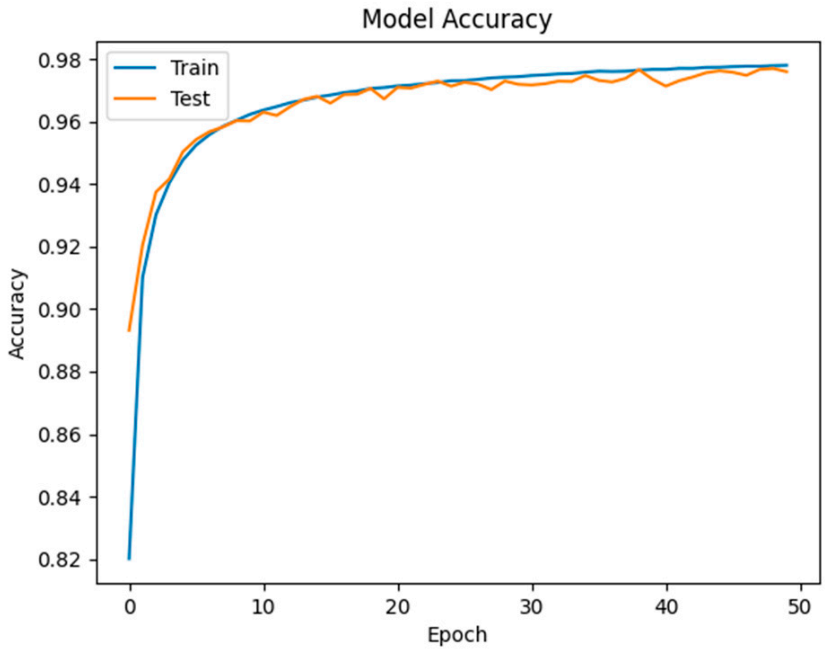

Figure 6. BDGN model accuracy.

Figure 7 depicts the model loss plot, demonstrating a steady decline in loss over the training iterations. The descending trajectory of the loss curve signifies the model's ability to learn effectively and minimize errors. The model loss reached a minimal value of

0.5%, highlighting the robustness of the BDGN model in capturing intricate patterns and optimizing cognitive workload classification.

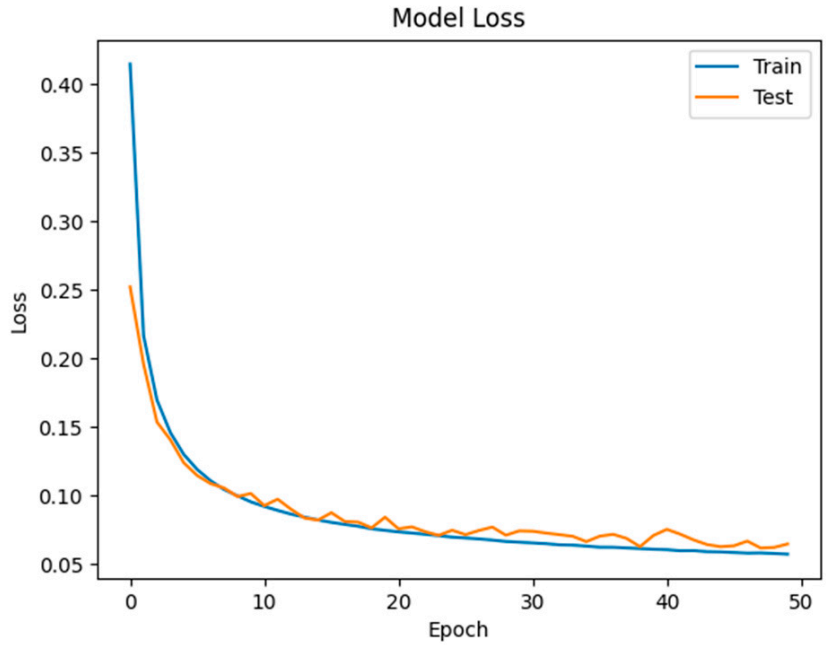

Figure 7. BDGN model loss.

The confusion matrix provides valuable insights into the BDGN model's classification performance across the different cognitive workload classes. The matrix comprises both diagonal elements, representing correctly classified instances, and off-diagonal elements, indicating misclassified instances. The confusion matrix is shown in Figure 8 to further evaluate the model's performance.

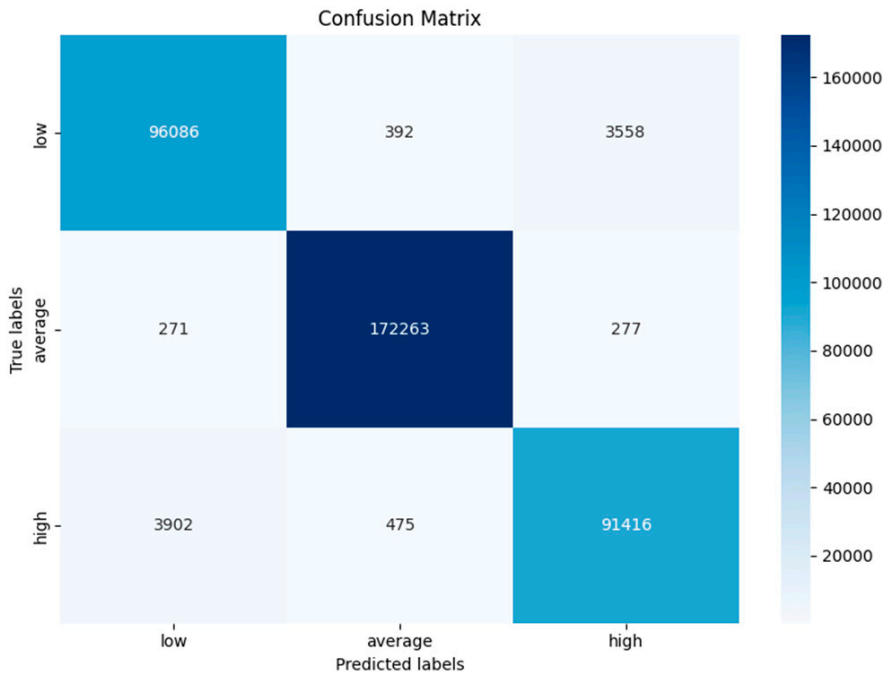

Figure 8. Confusion matrix showing all the labels.

Analyzing the specific values of the confusion matrix, we observe the following:

- The BDGN model accurately classified 96,086 instances as "Low Workload".
- For the "Medium-Workload" class, the model correctly classified 172,263 instances.
- In the "High-" class, the BDGN model achieved accurate classifications in 91,416 instances.

The confusion matrix values reveal the misclassifications as follows:

- The model misclassified 392 instances, assigning them to the neighboring "Medium-Workload" class, which should have been classified as "Low Workload".
- Similarly, there were 271 instances misclassified as "Low Workload" when they should have been classified as "Medium Workload".
- Additionally, the model misclassified 3558 instances as "Medium Workload" that should have been classified as "High Workload".
- Lastly, there were 475 instances misclassified as "Low Workload" instead of being classified as "High Workload".

The evaluation metrics presented in Table 1 provide a comprehensive analysis of the BDGN model's classification performance. These metrics include precision, recall, and F1-score, which offer insights into the model's accuracy, ability to capture relevant instances, and the balance between precision and recall.

Table 1. Evaluation metrics.

Labels	Precision	Recall	F1-Score
High	0.96	0.96	0.96
Low	0.99	1.00	1.00
Normal	0.96	0.95	0.96

The precision values obtained for each class are as follows:

- For the "High" class, the model achieved a precision of 0.96, indicating that 96% of instances classified as "High" were correctly identified.
- Similarly, the "Low" class attained a precision of 0.99, suggesting that 99% of instances classified as "Low" were accurately identified.
- For the "Normal" class, the model achieved a precision of 0.96, indicating that 96% of instances classified as "Normal" were correctly identified.

The recall values obtained for each class are as follows:

- The "High" class achieved a recall of 0.96, indicating that the model correctly identified 96% of the actual "High" workload instances.
- The "Low" class achieved a recall of 1.00, indicating that the model successfully identified all "Low" workload instances.
- The "Normal" class attained a recall of 0.95, signifying that 95% of the actual "Normal" workload instances were correctly identified.

The F1-scores obtained for each class are as follows:

- The "High" class achieved an F1-score of 0.96, indicating a balanced performance in terms of precision and recall.
- The "Low" class attained a perfect F1-score of 1.00, highlighting the model's ability to achieve a harmonious balance between precision and recall.
- The "Normal" class achieved an F1-score of 0.96, signifying a balanced performance similar to that for the "High" workload class.

4.2. Comparison with Existing Studies

We conducted a comparative analysis with existing studies in the field, as summarized in Table 2. Our study surpasses previous works in terms of accuracy, demonstrating the superiority of the BDGN model for cognitive workload classification. This comparison provides strong evidence of the model's effectiveness and reinforces its potential for practical implementation.

Table 2. Comparison with existing studies.

Paper	Year	Dataset	Classifier	Metric	Metric Value
[23]	2020	STEW	BLSTM-LSTM	Accuracy	82.57%
[33]	2023	STEW	Bi-LSTM and ResNet	Accuracy	90.64%
[34]	2021	Lab Experiment	Conv-LSTM	Accuracy	93.75%
[35]	2020	Lab Experiment	LSTM	Accuracy	90.8%
[36]	2019	Lab Experiment	SVM Decision Tree KNN Random forest	Accuracy	82.9% 70.4% 91.5% 84.6%
This Study	2023	STEW	Bi-directional Gated Network	Accuracy	98%

4.3. Real-Time Transmission and Classification

We implemented a data transmission system utilizing the MQTT (Message Queuing Telemetry Transport) protocol, maintaining a precise 1- to 3-millisecond transmission latency. MQTT (Message Queuing Telemetry Transport) protocol offers low-latency data transmission, typically with latencies ranging from 1 to 5 milliseconds, depending on network and implementation factors [48]. Our classification process involves accurately analyzing 128 signals across 14 channels, with each signal introducing a 1 s delay. The classification model operates within a 3 to 5 s timeframe. Thus, the entire classification procedure spans 132 to 134 s, showcasing our commitment to efficient and accurate analysis within this system.

The system consisted of a North Gateway, an MQTT broker, a Server, and a South Gateway. Figure 9 illustrates the MQTT Explorer with the Predicted Label set at high.

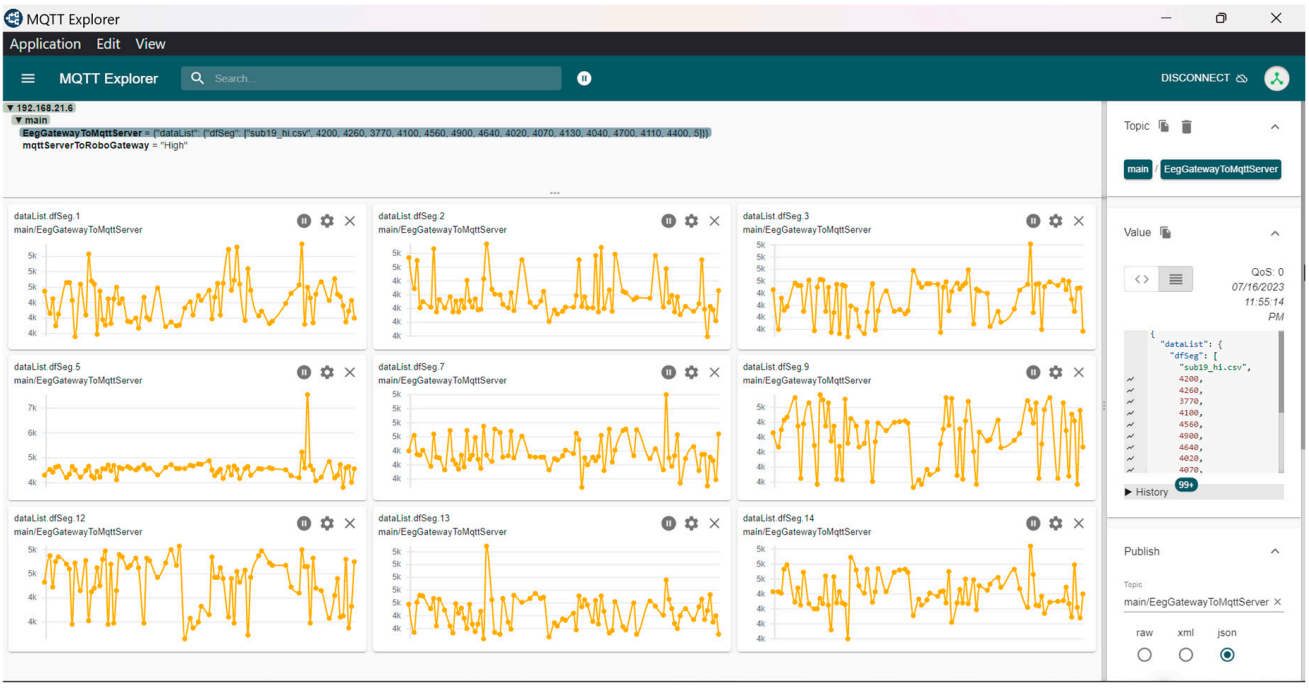

Figure 9. MQTT Explorer displays 9 segments of EEG data in separate windows with predicted classification as "High".

In Figure 10, the North Gateway shows the live reception of EEG (electroencephalography) data, ensuring a continuous flow of real-time data for classification.

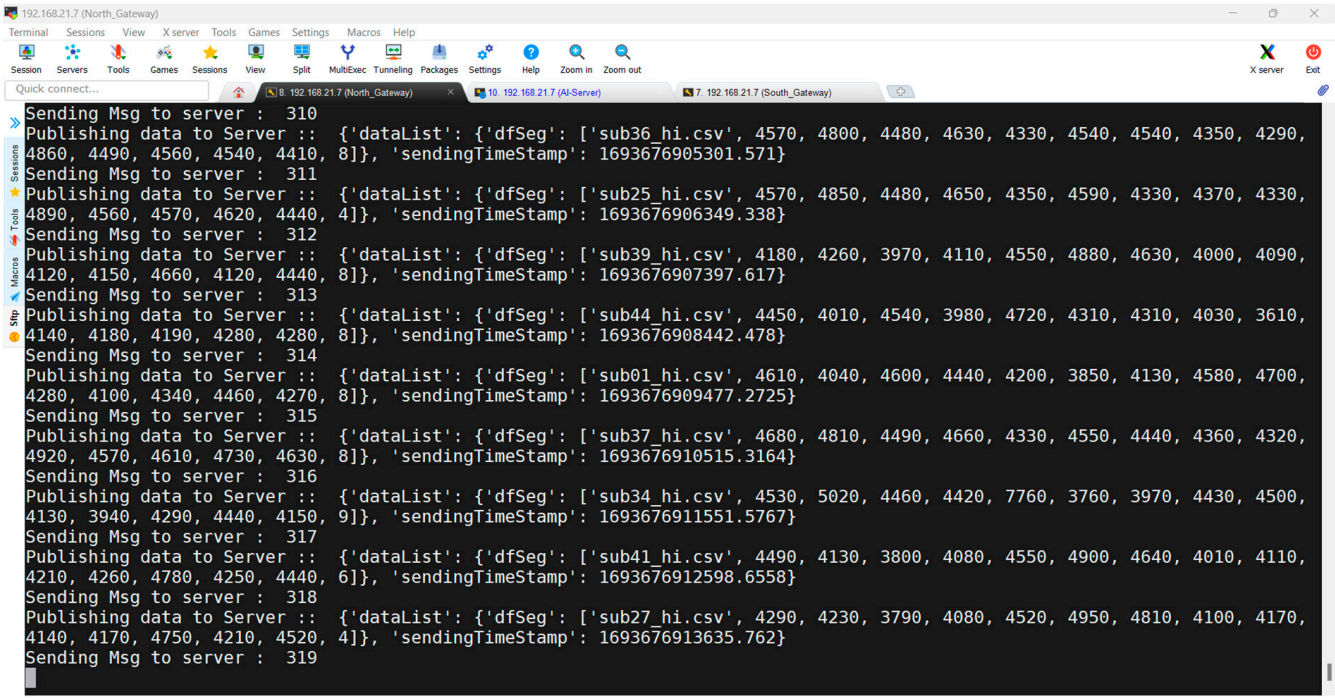

Figure 10. North Gateway showing live reception of EEG data.

The Server is a vital system component for performing real-time classification of cognitive workload levels. Leveraging the trained BDGN model, the Server processes the incoming EEG (electroencephalography) data and generates accurate predictions in real time. Figure 11 presents the integration of the Server within the MQTT-based system, which enables efficient cognitive workload classification. It receives live EEG data transmitted by the North Gateway and applies advanced algorithms to classify the cognitive workload levels of the users in real time.

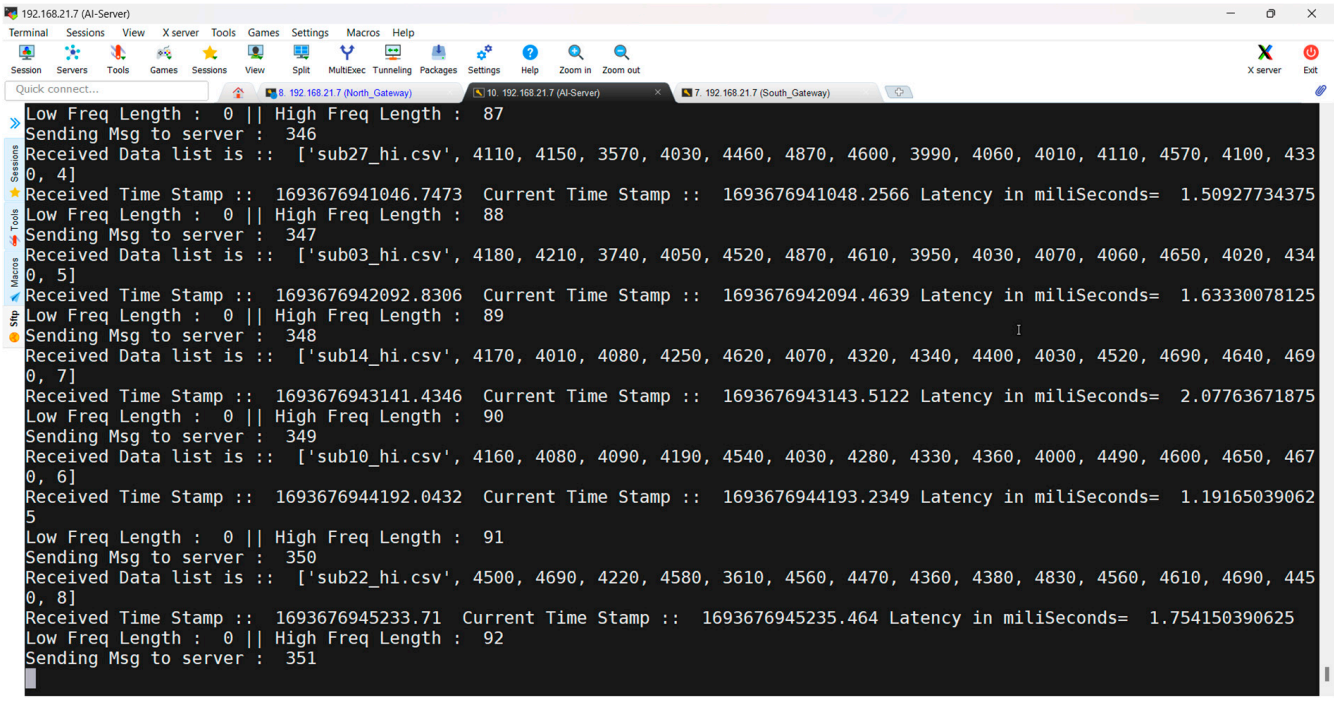

Figure 11. Server receiving live data from MQTT broker with transmission latency.

The South Gateway presents the classification results received from the server. Figure 12 visualizes the successful transmission of real-time classification information from the server to the South Gateway. The displayed results facilitate timely decision-making and intervention based on the user's cognitive workload level.

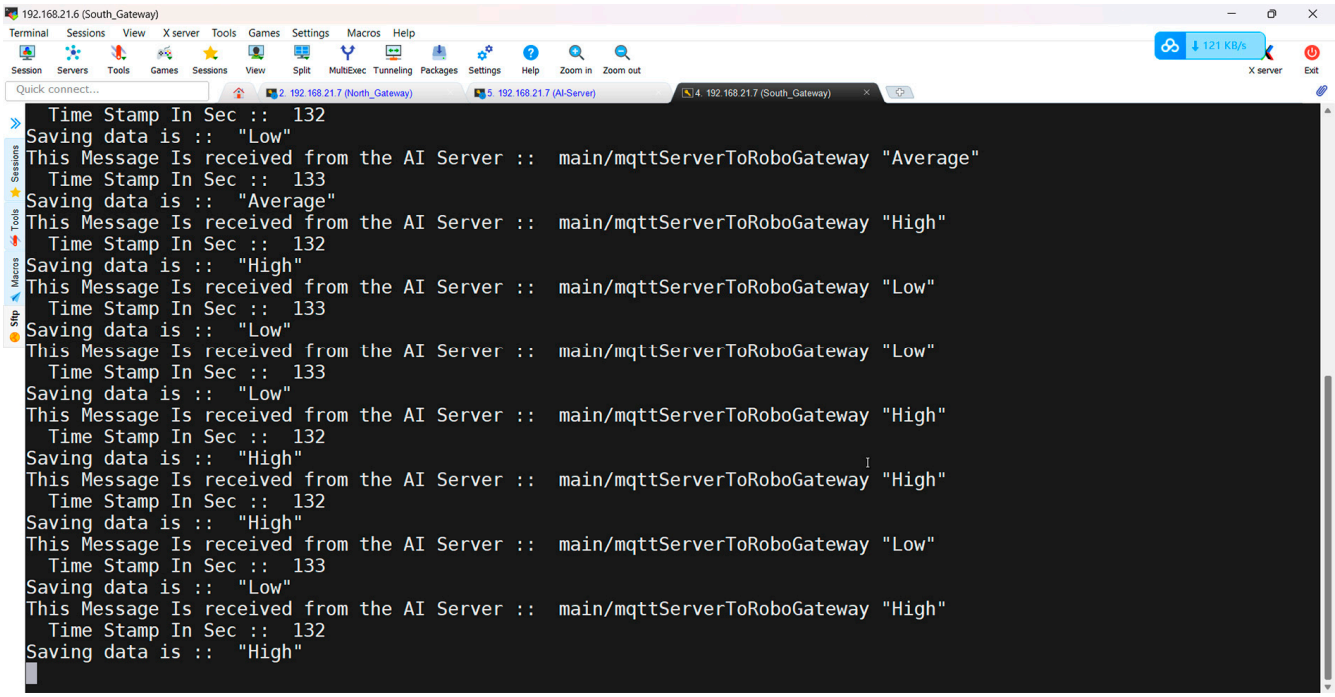

Figure 12. South Gateway showing real-time classification results from server with classification time in seconds.

These visualizations collectively illustrate the effectiveness and real-time nature of the proposed system. Integrating the BDGN model with the MQTT infrastructure enables continuous data transmission, real-time classification, and efficient dissemination of classification results. The real-time classification process ensures the prompt identification and monitoring of cognitive workload levels, enabling proactive measures to optimize performance, ensure safety, and enhance overall productivity in various Industry 5.0 applications. This simulation-based framework, uniting the BDGN model with MQTT technology, presents an avenue to practical implementation in real-world scenarios. While our study unfolds within a simulated environment, it beckons an exploration of its viability beyond digital confines. Our simulation identifies key metrics that extend their significance from simulation to reality. Table 3 provides a way of comparison and metrics including latency, classification accuracy, speed, and message loss rate serve as pivotal benchmarks for feasibility.

Table 3. Way to compare with real-world scenarios.

Metrics	This Study	Real-World Scenario
Latency in Data Transmission	1–3 ms	More than 100 ms
Accuracy of Classification	98%	Fed real-world data
Classification Speed	133 s	Data transmission delay will increase the classification time
Message Loss Rate	0	Depends on factors like distance, obstacles, interference, and signal strength

Our simulation reveals a latency of 1 to 3 milliseconds, whereas real-world latencies could surpass 100 milliseconds due to network dynamics. Classification accuracy at 98% in simulation aligns with real-world potential, though classification speed may change due to transmission delays. Additionally, our simulation reports a zero message loss rate, even though real-world rates hinge on factors like distance and signal strength. These metrics illuminate our framework's initial potential, while further validation through real-world data, comparative analysis, and sensitivity testing will bridge the gap between simulation and reality.

5. Conclusions and Future Research

In this study, our successful attempt at the classification of cognitive workload using EEG data yielded an impressive accuracy of 98% through the implementation of the BDGN model. The STEW dataset underwent preprocessing and was subjected to both time domain and power spectral density (PSD) analysis to enhance its suitability. Employing the MQTT protocol, the BDGN model was deployed to achieve real-time cognitive workload classification. These results underscore the potential of EEG-based cognitive workload classification utilizing the BDGN model. The achieved high accuracy substantiates the effectiveness of this approach in precisely discerning cognitive workload levels. Notably, our comparative analysis against state-of-the-art methodologies highlights the superiority of the recommended approach.

This research significantly advances the field of cognitive workload assessment and simultaneously unveils a roadmap for future exploration. Among the potential avenues, one promising trajectory involves deploying this classification system within industrial settings. We advocate for the integration of EEG devices endowed with Bluetooth-based wireless communication capabilities [49] for continuous real-time EEG data collection. In this envisioned direction, Raspberry Pi modules emerge as optimal hardware gateways [50], facilitating the streamlined transmission of EEG data from the source to the MQTT broker. Subsequently, the BDGN model deployed on the server effectively classifies the EEG data, and predictions are relayed by the MQTT broker. These predictions serve as the basis for instructing machines or robots via gateways, thus orchestrating work tasks in response to cognitive workload dynamics. This solution presents an economical means to implement cognitive workload classification within the Industry 5.0 context, promising enhanced operational efficiency and adaptability. As we embark on these promising trajectories, the fusion of advanced technology and cognitive assessment holds the potential to reshape industrial processes in impactful ways.

However, this study acknowledges several limitations. Firstly, the reliance on a specific dataset could limit the broader applicability of findings across diverse populations and contexts. Variations in electrode placement during EEG data collection may introduce inconsistencies, impacting model robustness. While the focus is on cognitive workload, external factors influencing EEG signals, like environmental conditions, remain underexplored. The hybrid architecture of the BDGN approach, while accurate, might pose implementation and interpretability challenges due to complexity. Although emphasizing Industry 5.0 relevance, the direct transferability of findings to other domains necessitates further investigation. Addressing these limitations in future research could yield a more universally applicable cognitive workload classification approach. Additionally, exploring BDGN model generalizability and scalability across diverse datasets, domains, and populations, as well as integrating other physiological and contextual features, will enhance the understanding of cognitive workload.

Author Contributions: Conceptualization, M.A.A. and B.A.; methodology, M.A.A., B.A. and S.U.B.; software, M.A.A.; data curation, M.A.A. and S.U.B.; writing—original draft preparation, M.A.A.; writing—review and editing, M.A.A., Z.G., B.A. and S.U.B.; visualization, M.A.A. and S.U.B.; supervision, Z.G. All authors have read and agreed to the published version of the manuscript.

Funding: This research received no external funding.

Data Availability Statement: Data available in a publically accessible repository.

Conflicts of Interest: The authors declare no conflict of interest.

References

1. Dev, K.; Tsang, K.F.; Rodríguez, J.M.C. Guest Editorial: The Era of Industry 5.0—Technologies from No Recognizable HM Interface to Hearty Touch Personal Products. *IEEE Trans. Ind. Inform.* **2022**, *18*, 5432–5434. [CrossRef]
2. Prassida, G.F.; Asfari, U. A Conceptual Model for the Acceptance of Collaborative Robots in Industry 5.0. *Procedia Comput. Sci.* **2022**, *197*, 61–67. [CrossRef]
3. Lin, C.J.; Lukodono, R.P. Classification of mental workload in Human-robot collaboration using machine learning based on physiological feedback. *J. Manuf. Syst.* **2022**, *65*, 673–685. [CrossRef]
4. Panchetti, T.; Pietrantoni, L.; Puzzo, G.; Gualtieri, L.; Fraboni, F. Assessing the Relationship between Cognitive Workload, Workstation Design, User Acceptance and Trust in Collaborative Robots. *Appl. Sci.* **2023**, *13*, 1720. [CrossRef]
5. Longo, L.; Wickens, C.D.; Hancock, G.; Hancock, P.A. Human Mental Workload: A Survey and a Novel Inclusive Definition. *Front. Psychol.* **2022**, *13*, 883321, Erratum in *Front. Psychol.* **2022**, *13*, 969140. [CrossRef]
6. Chen, O.; Paas, F.; Sweller, J. A Cognitive Load Theory Approach to Defining and Measuring Task Complexity Through Element Interactivity. *Educ. Psychol. Rev.* **2023**, *35*, 63. [CrossRef]
7. Faure, V.; Lobjois, R.; Benguigui, N. The Effects of Driving Environment Complexity and Dual Tasking on Drivers' Mental Workload and Eye Blink Behavior. *Transp. Res. Part F Traffic Psychol. Behav.* **2016**, *40*, 78–90. [CrossRef]
8. Fan, J.; Smith, A.P. The Impact of Workload and Fatigue on Performance. In *Human Mental Workload: Models and Applications*; Springer International Publishing: Berlin/Heidelberg, Germany, 2017; pp. 90–105. [CrossRef]
9. Wang, H.; Lv, L.; Li, X.; Li, H.; Leng, J.; Zhang, Y.; Thomson, V.; Liu, G.; Wen, X.; Sun, C.; et al. A Safety Management Approach for Industry 5.0's Human-Centered Manufacturing Based on Digital Twin. *J. Manuf. Syst.* **2023**, *66*, 1–12. [CrossRef]
10. Aygun, A.; Nguyen, T.; Haga, Z.; Aeron, S.; Scheutz, M. Investigating Methods for Cognitive Workload Estimation for Assistive Robots. *Sensors* **2022**, *22*, 6834. [CrossRef] [PubMed]
11. Rajasekharan, H.; Chivilkar, S.; Bramhankar, N.; Sharma, T.; Daruwala, R. EEG-based Mental Workload Assessment using a Graph Attention Network. In Proceedings of the 2021 IEEE 20th International Conference on Cognitive Informatics & Cognitive Computing (ICCI*CC), Banff, AB, Canada, 29–31 October 2021; pp. 78–84. [CrossRef]
12. Chanel, P.C.C.; Wilson, M.D.; Scannella, S. Online ECG-based Features for Cognitive Load Assessment. In Proceedings of the 2019 IEEE International Conference on Systems, Man and Cybernetics (SMC), Bari, Italy, 6–9 October 2019; pp. 3710–3717. [CrossRef]
13. Park, J.; Zahabi, M. Comparison of Cognitive Workload Assessment Techniques in EMG-based Prosthetic Device Studies. In Proceedings of the 2020 IEEE International Conference on Systems, Man, and Cybernetics (SMC), Toronto, ON, Canada, 11–14 October 2020; pp. 1242–1248. [CrossRef]
14. Bozkir, E.; Geisler, D.; Kasneci, E. Person Independent, Privacy Preserving, and Real Time Assessment of Cognitive Load using Eye Tracking in a Virtual Reality Setup. In Proceedings of the 2019 IEEE Conference on Virtual Reality and 3D User Interfaces (VR), Osaka, Japan, 23–27 March 2019; pp. 1834–1837. [CrossRef]
15. Knisely, B.M.; Joyner, J.S.; Vaughn-Cooke, M. Cognitive task analysis and workload classification. *MethodsX* **2021**, *8*, 101235. [CrossRef] [PubMed]
16. Karmakar, S.; Kamilya, S.; Dey, P.; Guhathakurta, P.K.; Dalui, M.; Bera, T.K.; Halder, S.; Koley, C.; Pal, T.; Basu, A. Real time detection of cognitive load using fNIRS: A deep learning approach. *Biomed. Signal Process. Control* **2023**, *80*, 104227. [CrossRef]
17. Shriram, R.; Sundhararajan, M.; Daimiwal, N. EEG Based Cognitive Workload Assessment for Maximum Efficiency. *IOSR J. Electron. Commun. Eng. (IOSR-JECE)* **2012**, *7*, 34–38.
18. Antoniades, A.; Spyrou, L.; Took, C.C.; Sanei, S. Deep learning for epileptic intracranial EEG data. In Proceedings of the 2016 IEEE 26th International Workshop on Machine Learning for Signal Processing (MLSP), Vietri sul Mare, Italy, 13–16 September 2016; pp. 1–6. [CrossRef]
19. Vortmann, L.-M.; Kroll, F.; Putze, F. EEG-Based Classification of Internally- and Externally-Directed Attention in an Augmented Reality Paradigm. *Front. Hum. Neurosci.* **2019**, *13*, 348. [CrossRef]
20. Light, G.A.; Williams, L.E.; Minow, F.; Sprock, J.; Rissling, A.; Sharp, R.; Swerdlow, N.R.; Braff, D.L. Electroencephalography (EEG) and event-related potentials (ERPs) with human participants. *Curr. Protoc. Neurosci.* **2010**, *52*, 6–25. [CrossRef] [PubMed]
21. Asgher, U.; Khalil, K.; Ayaz, Y.; Ahmad, R.; Khan, M.J. Classification of Mental Workload (MWL) using Support Vector Machines (SVM) and Convolutional Neural Networks (CNN). In Proceedings of the 2020 3rd International Conference on Computing, Mathematics and Engineering Technologies (iCoMET), Sukkur, Pakistan, 29–30 January 2020; pp. 1–6. [CrossRef]
22. Gallardo-Antolín, A.; Montero, J.M. Interspeech 2019. In Proceedings of the 20th Annual Conference of the International Speech Communication Association, Graz, Austria, 15–19 September 2019; ISCA: New York, NY, USA, 2019; pp. 216–220. [CrossRef]
23. Chakladar, D.D.; Dey, S.; Roy, P.P.; Dogra, D.P. EEG-based mental workload estimation using deep BLSTM-LSTM network and evolutionary algorithm. *Biomed. Signal Process. Control.* **2020**, *60*, 101989. [CrossRef]
24. Cao, Z. A review of artificial intelligence for EEG-based brain−computer interfaces and applications. *Brain Sci. Adv.* **2020**, *6*, 162–170. [CrossRef]

25. Mahara, G.S.; Gangele, S. Fake news detection: A RNN-LSTM, Bi-LSTM based deep learning approach. In Proceedings of the 2022 IEEE 1st International Conference on Data, Decision and Systems (ICDDS), Bangalore, India, 2–3 December 2022; pp. 1–6. [CrossRef]
26. Pavithra, M.; Saruladha, K.; Sathyabama, K. GRU Based Deep Learning Model for Prognosis Prediction of Disease Progression. In Proceedings of the 2019 3rd International Conference on Computing Methodologies and Communication (ICCMC), Erode, India, 27–29 March 2019; pp. 840–844. [CrossRef]
27. IEEE Dataport. STEW: Simultaneous Task EEG Workload Dataset. Available online: https://ieee-dataport.org/open-access/stew-simultaneous-task-eeg-workload-dataset (accessed on 25 April 2023).
28. Hasan, H.; Mohammed, B. Evaluation of MQTT Protocol for IoT Based Industrial Automation. *Int. J. Eng. Sci. Comput.* **2018**, *8*, 19364–19369.
29. Silva, D.R.C.; Oliveira, G.M.B.; Silva, I.; Ferrari, P.; Sisinni, E. Latency evaluation for MQTT and WebSocket Protocols: An Industry 4.0 perspective. In Proceedings of the 2018 IEEE Symposium on Computers and Communications (ISCC), Natal, Brazil, 25–28 June 2018; pp. 01233–01238. [CrossRef]
30. Atmoko, R.; Riantini, R.; Hasin, M.K. IoT real time data acquisition using MQTT protocol. *J. Phys. Conf. Ser.* **2017**, *853*, 012003. [CrossRef]
31. Liu, R.; Qi, S.; Hao, S.; Lian, G.; Luo, Y. Using electroencephalography to analyse drivers' different cognitive workload characteristics based on on-road experiment. *Front. Psychol.* **2023**, *14*, 1107176. [CrossRef]
32. Yang, J.; Liu, T.; Liu, Y.; Morgan, P. Review of Human-Machine Interaction Towards Industry 5.0: Human-Centric Smart Manufacturing. In Proceedings of the International Design Engineering Technical Conferences and Computers and Information in Engineering Conference, St. Louis, MO, USA, 14–17 August 2022; American Society of Mechanical Engineers: New York, NY, USA, 2022. [CrossRef]
33. Shao, S.; Han, G.; Wang, T.; Lin, C.; Song, C.; Yao, C. EEG-Based Mental Workload Classification Method Based on Hybrid Deep Learning Model Under IoT. *IEEE J. Biomed. Health Inform.* **2023**. [CrossRef]
34. Gupta, A.; Siddhad, G.; Pandey, V.; Roy, P.P.; Kim, B.-G. Subject-Specific Cognitive Workload Classification Using EEG-Based Functional Connectivity and Deep Learning. *Sensors* **2021**, *21*, 6710. [CrossRef] [PubMed]
35. Kwak, Y.; Kong, K.; Song, W.-J.; Min, B.-K.; Kim, S.-E. Multilevel Feature Fusion With 3D Convolutional Neural Network for EEG-Based Workload Estimation. *IEEE Access* **2020**, *8*, 16009–16021. [CrossRef]
36. Plechawska-Wójcik, M.; Tokovarov, M.; Kaczorowska, M.; Zapała, D. A Three-Class Classification of Cognitive Workload Based on EEG Spectral Data. *Appl. Sci.* **2019**, *9*, 5340. [CrossRef]
37. Teymourlouei, A.; Gentili, R.J.; Reggia, J. Decoding EEG Signals with Visibility Graphs to Predict Varying Levels of Mental Workload. In Proceedings of the 2023 57th Annual Conference on Information Sciences and Systems (CISS), Baltimore, MD, USA, 22–24 March 2023; pp. 1–6. [CrossRef]
38. Ahmad, A.; Darmoul, S.; Dabwan, A.; Alkahtani, M.; Samman, S. Human error in multitasking environments. In Proceedings of the 6th International Conference on Industrial Engineering and Operations Management (IEOM 2016), Kuala Lumpur, Malaysia, 8–10 March 2016; pp. 1265–1272.
39. Kwak, S.Y.H.N.S.; Taegeun, O.; Seong, W.L. Classification of pilots' mental states using a multimodal deep learning network. *Biocybern. Biomed. Eng.* **2020**, *40*, 324–336.
40. Guerrero, L.-D.; Romero, L.D.; Bueno-López, M. A review of epileptic seizure detection using EEG signals analysis in the time and frequency domain. In Proceedings of the 2021 IEEE 21st International Conference on Communication Technology (ICCT), Tianjin, China, 13–16 October 2021; pp. 1363–1367. [CrossRef]
41. Qin, X.; Zheng, Y.; Chen, B. Extract EEG Features by Combining Power Spectral Density and Correntropy Spectral Density. In Proceedings of the 2019 Chinese Automation Congress (CAC), Hangzhou, China, 22–24 November 2019; pp. 2455–2459. [CrossRef]
42. Delimayanti, M.K.; Purnama, B.; Nguyen, N.G.; Faisal, M.R.; Mahmudah, K.R.; Indriani, F.; Kubo, M.; Satou, K. Classification of Brainwaves for Sleep Stages by High-Dimensional FFT Features from EEG Signals. *Appl. Sci.* **2020**, *10*, 1797. [CrossRef]
43. Abid, M.A.; Ullah, S.; Siddique, M.A.; Mushtaq, M.F.; Aljedaani, W.; Rustam, F. Spam SMS filtering based on text features and supervised machine learning techniques. *Multimed. Tools Appl.* **2022**, *81*, 39853–39871. [CrossRef]
44. Amaar, A.; Aljedaani, W.; Rustam, F.; Ullah, S.; Rupapara, V.; Ludi, S. Detection of fake job postings by utilizing machine learning and natural language processing approaches. *Neural Process. Lett.* **2022**, *54*, 2219–2247. [CrossRef]
45. Rupapara, V.; Rustam, F.; Aljedaani, W.; Shahzad, H.F.; Lee, E.; Ashraf, I. Blood cancer prediction using leukemia microarray gene data and hybrid logistic vector trees model. *Sci. Rep.* **2022**, *12*, 1000. [CrossRef]
46. Fang, F.; Wu, J.; Li, Y.; Ye, X.; Aljedaani, W.; Mkaouer, M.W. On the classification of bug reports to improve bug localization. *Soft Comput.* **2021**, *25*, 7307–7323. [CrossRef]
47. Govindan, K.; Azad, A.P. End-to-end service assurance in IoT MQTT-SN. In Proceedings of the 2015 12th Annual IEEE Consumer Communications and Networking Conference (CCNC), Las Vegas, NV, USA, 9–12 January 2015; pp. 290–296. [CrossRef]
48. EMQ X. EMQ X Documentation. Available online: https://www.emqx.io/docs/en/v5/ (accessed on 31 August 2023).

49. Lovelace, J.A.; Witt, T.S.; Beyette, F.R. Modular, bluetooth enabled, wireless electroencephalograph (EEG) platform. In Proceedings of the 2013 35th Annual International Conference of the IEEE Engineering in Medicine and Biology Society (EMBC), Osaka, Japan, 3–7 July 2013; pp. 6361–6364. [CrossRef]
50. Chen, H.; Jia, X.; Li, H. A brief introduction to IoT gateway. In Proceedings of the IET International Conference on Communication Technology and Application (ICCTA 2011), Beijing, China, 14–16 October 2011; pp. 610–613. [CrossRef]